

# Hydrolysis protection and sintering of aluminum nitride powders with yttria nanofilms

Rebecca J. O'Toole<sup>1</sup>  | Chanel Hill<sup>1</sup> | Peter J. Buur<sup>1</sup> | Christopher J. Bartel<sup>1</sup> |  
Christopher J. Gump<sup>2</sup> | Charles B. Musgrave<sup>1,3,4,5</sup> | Alan W. Weimer<sup>1</sup> 

<sup>1</sup> Department of Chemical and Biological Engineering, University of Colorado Boulder, Boulder, Colorado, USA

<sup>2</sup> Forge Nano, Inc., Thornton, Colorado, USA

<sup>3</sup> Department of Chemistry, University of Colorado Boulder, Boulder, Colorado, USA

<sup>4</sup> Materials Science and Engineering Program, University of Colorado Boulder, Boulder, Colorado, USA

<sup>5</sup> Materials and Chemical Science and Technology, National Renewable Energy Laboratory, Golden, Colorado, USA

## Correspondence

Alan W. Weimer, Department of Chemical and Biological Engineering, University of Colorado Boulder, Boulder, CO, 80309, USA.

Email: [alan.weimer@colorado.edu](mailto:alan.weimer@colorado.edu)

## Funding information

National Science Foundation, Grant/Award Number: 1563537

## Abstract

Aluminum nitride (AlN) is a promising material for electronic substrates and heat sinks. However, AlN powders react with water that adversely affects final part properties and necessitates processing in organic solvents, increasing the cost of AlN parts. Small quantities of yttrium oxide (Y<sub>2</sub>O<sub>3</sub>) are commonly added to AlN particles to enable liquid phase sintering. To mitigate the reaction of AlN particles with water, particle atomic layer deposition (ALD) was used to coat AlN powders with conformal films of Y<sub>2</sub>O<sub>3</sub> prior to densification and powder processing. When AlN particles were coated with 6 nm thick films of amorphous Y<sub>2</sub>O<sub>3</sub>, the hydrolysis reaction was significantly suppressed over 48 h, demonstrating that Y<sub>2</sub>O<sub>3</sub> nanofilms on AlN powders act as a barrier coating in an aqueous solution. AlN powders with Y<sub>2</sub>O<sub>3</sub> addition by particle ALD sintered to high relative densities ( $\geq 90\%$  theoretical) after sintering at 1800°C for 50 min.

## KEYWORDS

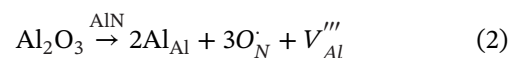
aluminum nitride, atomic layer deposition, environmental barrier coatings (EBC), sinter/sintering

## 1 | INTRODUCTION

A high thermal conductivity (150–200 W m<sup>-1</sup> K<sup>-1</sup>)<sup>1–3</sup> and low electronic conductivity make aluminum nitride (AlN) an ideal material for electronic heat sinks. Its thermal conductivity is much higher than most ceramic materials and is similar to that of metals.<sup>4</sup> However, AlN's low electronic conductivity enables the direct fabrication of integrated circuits on the heat sink, eliminating the dielectric layer needed to electrically isolate the metal heat sink from the LED.<sup>5,6</sup>

AlN has many desirable properties, but it is expensive to produce due to the high sintering temperatures required to reach near-theoretical density and reactivity with water.

AlN degrades in water, forming Al<sub>2</sub>O<sub>3</sub> that dissolves into the AlN lattice to produce vacancies on aluminum sites ( $V_{Al}'''$ )<sup>7–10</sup>:



These vacancies scatter phonons traveling through the lattice, thereby reducing the thermal conductivity.<sup>11,12</sup> To mitigate this reaction, AlN powders must be handled in organic solvents which increases processing costs.

AlN requires sintering temperatures of  $\sim 1800^\circ\text{C}$  to reach high densities, even with the addition of sintering aids. Conventionally, AlN densifies by liquid phase sintering with the addition of  $\text{Y}_2\text{O}_3$ ,<sup>1-3,13,14</sup>  $\text{CaO}$ ,<sup>14-16</sup> and/or other materials<sup>2,13,17,18</sup> as sintering aids. These secondary phases also react with  $\text{Al}_2\text{O}_3$  impurities produced during AlN powder synthesis, sequestering them to grain boundaries and triple points to avoid the formation of  $V_{\text{Al}}$  (Equation 2) and increasing the thermal conductivity.<sup>1,2</sup>

Typically, sintering aids are added by ball milling<sup>1,14,15,18-20</sup> or vibratory milling<sup>2,13</sup> of sintering aid particles with AlN powders. In this work, we propose a novel method of liquid phase sintering aid addition, particle atomic layer deposition (ALD). Particle ALD is a thin film deposition technique that uses sequential surface-limited reactions to grow thin films that are chemically bonded to the surface of substrate particles.<sup>21</sup> Here, particle ALD is used to add  $\text{Y}_2\text{O}_3$  to AlN particles as a conformal nanoscale surface coating, homogeneously dispersing the sintering aid prior to densification. Additionally, ALD-coated powders have shown reduced reactivity toward environmental species, including SiC in steam<sup>22</sup> and  $\text{ZrO}_2$  in  $\text{H}_2$ .<sup>23</sup> By adding the  $\text{Y}_2\text{O}_3$  as a nanofilm instead of particles, it acts as a barrier coating and protects the AlN particle surface from reaction with water to enable aqueous processing.

## 2 | EXPERIMENTAL SECTION

Commercial AlN powder (Tokuyama Soda, Grade E,  $3.4 \text{ m}^2/\text{g}$ ) was coated with nanoscale films of  $\text{Y}_2\text{O}_3$  in a fluidized bed reactor at  $300^\circ\text{C}$ . Nitrogen was used as the carrier gas. The yttrium precursor (Arya, Air Liquide) was supplied using a bubbler and oxygen was the oxygen source. Typically, after the precursor reacts with all available functional groups on the particle surface, "breakthrough" occurs where a characteristic atomic mass signal increases in the mass spectrometer, indicating that an unreacted precursor is flowing through the powder bed.<sup>24</sup> Precursor breakthrough was not observed when dosing the yttrium precursor, so it is unknown if the surface reaction reached completion. Therefore, the number of ALD cycles is not reported.

To characterize the composition of the ALD-coated powders, the yttrium content was determined by inductively coupled plasma-optical emission spectroscopy (ICP-OES), and LECO light element analysis (LECO TC600 and LECO C200) was used to determine carbon and oxygen content. Transmission electron microscopy (TEM; Tecnai ST20) was used to characterize the film.

For comparison to the ALD-coated powders, AlN powder samples with equivalent  $\text{Y}_2\text{O}_3$  content added by

TABLE 1  $\text{Y}_2\text{O}_3$  wt% and method of addition for all samples

Sample	$\text{Y}_2\text{O}_3$ content (wt %)	Addition method
0%ALD	0	NA
0.4%ALD	0.4	ALD
6.5%ALD	6.5	ALD
0.4%MIX	0.4	Mechanical mixing
6.5%MIX	6.5	Mechanical mixing

mechanical mixing were prepared (Table 1). AlN powder was mixed with 0.4 and 6.5 wt%  $\text{Y}_2\text{O}_3$  powder (Sigma Aldrich, 99.99% trace metal basis,  $3.3 \text{ m}^2/\text{g}$ ) for 24 h in a drum roller with isopropanol and yttria-tetragonally stabilized zirconia milling media (Tosoh) in a 10:1 media to powder ratio. The solvent was then removed by drying under vacuum for  $\sim 2$  days.

To characterize the hydrolysis behavior of coated and uncoated AlN powders, 1.5 g of 0%ALD, 0.4%ALD, and 6.5%ALD powders were placed in 150 ml of distilled water at  $30^\circ\text{C}$  under stirring. As the AlN powders react with water, ammonia is produced resulting in an increase in pH (Equations 1–2). The pH was monitored over  $\sim 48$  h using a pH meter (Sartorius) and was stored on a computer at various time intervals. Pure  $\text{Y}_2\text{O}_3$  powder (Sigma Aldrich, 99.99% trace metal basis,  $3.3 \text{ m}^2/\text{g}$ ) was also tested as a control.

All powders were mixed with 6 wt% polyethylene glycol (Alfa Aesar polyethylene glycol 8000) and isopropanol in a mortar and pestle. The mixture was then placed under a vacuum overnight for solvent removal. Then, the powder/binder mixture was placed in a stainless-steel die and pressed at 350 MPa for 90 s to form 6 mm diameter powder compacts. For each sintering experiment, the pellet was placed in a boron nitride protective sleeve. The temperature was then raised to  $600^\circ\text{C}$  at a rate of  $2^\circ\text{C}/\text{min}$  followed by a 10 min isothermal hold for the removal of binder and then from 600 to  $1800^\circ\text{C}$  at  $10^\circ\text{C}/\text{min}$  followed by a 50 min isothermal hold. After sintering, the final density of the specimen was determined by geometric measurement. A fracture surface of the dense samples was characterized using backscattered electron-scanning electron microscopy (BSE-SEM, Hitachi SU3500) with an accelerating voltage of 10 kV.

## 3 | RESULTS AND DISCUSSION

The  $\text{Y}_2\text{O}_3$  content determined by ICP-OES was 0, 0.4, and 6.5 wt%  $\text{Y}_2\text{O}_3$  for 0%ALD, 0.4%ALD, and 6.5%ALD, respectively, where the wt%  $\text{Y}_2\text{O}_3$  is denoted in the sample name (Table 1). The uncoated AlN powder had an oxygen and carbon content of  $1.2 \pm 0.2$  and  $0.13 \pm 0.01$  wt%,

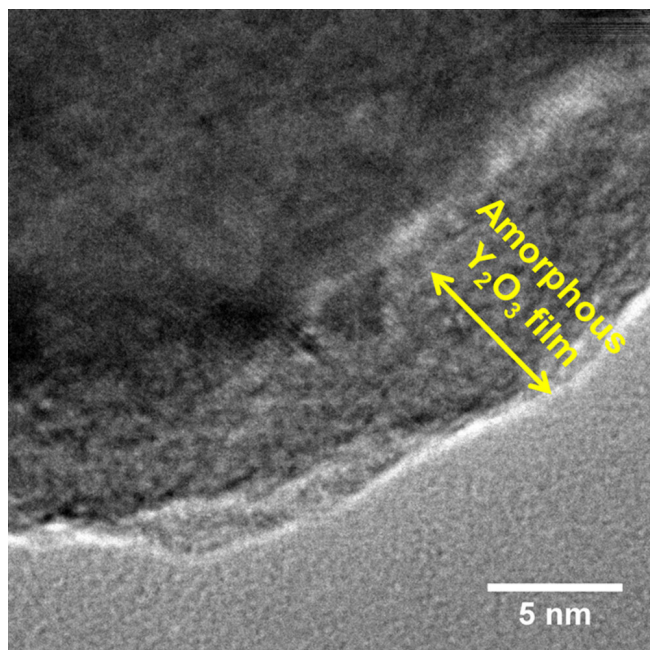


**FIGURE 1** Transmission electron microscopy (TEM) of aluminum nitride (AlN) powder with 6.5 wt%  $Y_2O_3$  added by particle ALD, where the AlN particle is coated with an amorphous film of  $Y_2O_3$  that is  $\sim 6$  nm in thickness

respectively, as determined by LECO light element analysis. For 6.5%ALD, the carbon content after the ALD process increased to  $0.41 \pm 0.02$  wt%, showing that some carbon impurities are present in the film. TEM was used to characterize the  $Y_2O_3$  film of 6.5%ALD (Figure 1). The lattice of the AlN particles is apparent, and the AlN particles were coated with conformal thin films of amorphous  $Y_2O_3$ . The film thickness was  $\sim 6$  nm with 6.5 wt%  $Y_2O_3$  addition.

The hydrolysis behavior of the uncoated powders was measured by determining the change in pH over time of a water/powder mixture (Equation 1). The pH of 0%ALD increases quickly from 6 to  $\sim 10.5$  over 10 h, suggesting that the uncoated powder quickly hydrolyzes in the presence of water (Figure 2). After 10 h, the pH decreases possibly due to the volatilization of  $NH_3$  from the solution. The pH of 0.4%ALD reaches  $\sim 8.25$  after 48 h, suggesting that adding a  $Y_2O_3$  nanofilm by particle ALD suppresses the hydrolysis reaction. However, a gradual increase in pH is observed over the first 10 h, suggesting that the film is incomplete with only 0.4 wt%  $Y_2O_3$  addition.

With 6.5 wt%  $Y_2O_3$  addition, the final pH is  $\sim 7.6$  after 48 h, less than the final pH of both 0%ALD and 0.4%ALD. The hydrolysis behavior of 6.5%ALD more closely resembles that of pure- $Y_2O_3$ , suggesting that the  $Y_2O_3$  film effectively protects the surface of the particles from reaction with water. However, the pH of 6.5%ALD still increases slightly from 7 to 7.6 over 48 h. This is likely because of the slow dissolution of the amorphous  $Y_2O_3$  film into solu-

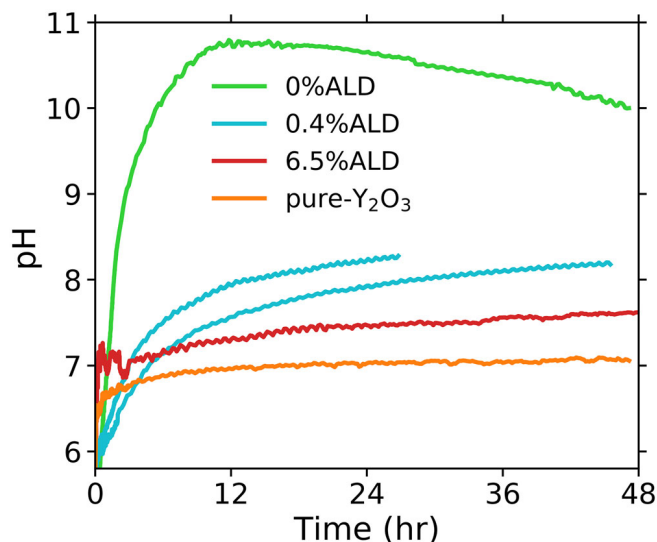


**FIGURE 2** The hydrolysis behavior of the uncoated and ALD-coated aluminum nitride (AlN) powders, along with pure- $Y_2O_3$  powder run as a control. The addition of 6.5 wt%  $Y_2O_3$  by particle ALD significantly reduces AlN hydrolysis over  $\sim 48$  h

tion, as some amorphous ceramics have limited solubility in water at relatively low temperatures.<sup>25,26</sup> This slowly creates porosity in the film, as reported previously for amorphous  $Al_2O_3$  films in water.<sup>25</sup>

For 0%ALD, only 70% theoretical density was achieved after sintering. When a small quantity of  $Y_2O_3$  is added ( $\geq 0.4$  wt%) by ALD or mechanical mixing, all samples reach high densities that are  $\geq 90\%$  theoretical. The fracture surfaces of dense samples were characterized by BSE-SEM (Figure 3). In samples with 6.5 wt%  $Y_2O_3$ , the  $Y_2O_3$  phase migrated significantly as the  $Y_2O_3$  is not uniformly distributed throughout the final microstructure. The addition of  $Y_2O_3$  by both mechanical mixing and particle ALD leads to a non-uniform distribution of the secondary phase at this concentration.

## 4 | CONCLUSION

Particle atomic layer deposition (ALD) was used to coat AlN powders with conformal thin films of amorphous  $Y_2O_3$ , demonstrating a novel method for the addition of liquid phase sintering aids to AlN powders. Hydrolysis experiments revealed that an  $\sim 6$  nm  $Y_2O_3$  film (6.5 wt%) significantly reduced the hydrolysis of the AlN particles over 48 h, illustrating that deposition of  $Y_2O_3$  nanofilms on AlN particles by ALD protects the AlN particle surface from hydrolysis. However, a gradual increase in pH over this time interval suggested that the amorphous  $Y_2O_3$  slowly dissolved in water to form porosity.

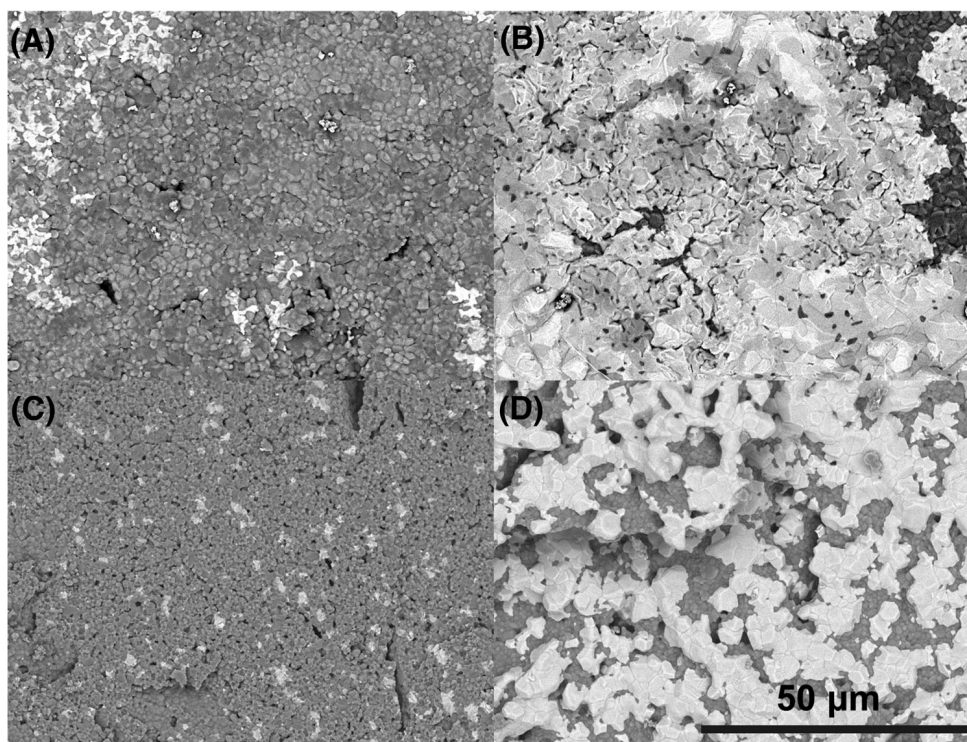


FIGURE 3 Micrograph of (A–B) 6.5%ALD and (C–D) 6.5%MIX in two different locations. The gray grains are AlN and the white phase is  $Y_2O_3$  which is non-homogeneously dispersed after sintering

Samples with  $Y_2O_3$  addition by either mechanical mixing or particle ALD achieved  $\geq 90\%$  relative density after sintering at  $1800^\circ C$  and contained a non-uniformly dispersed  $Y_2O_3$  phase throughout the microstructure.

#### ACKNOWLEDGMENTS

The authors are grateful for the support of the National Science Foundation (GOALI #1563537) and RO is grateful for financial support provided by the Teet's fellowship (University of Colorado Boulder). The authors also thank Fredrick Luiszer (University of Colorado Boulder) for performing ICP analysis, COSINC for SEM access (CU Boulder), Dr. Sarah Bull for assistance with TEM, and FEMM for TEM access (CU Boulder).

#### CONFLICT OF INTEREST

A.W. Weimer has a significant financial interest in Forge Nano, Inc.

#### ORCID

Rebecca J. O'Toole  <https://orcid.org/0000-0001-8785-206X>

Alan W. Weimer  <https://orcid.org/0000-0002-2471-349X>

#### REFERENCES

1. Lee WE, Chiang SK, Readey DW, Donn R, Shaffer PTB. Relation between thermal conductivity, sintering mechanism and microstructure of AlN with yttrium aluminate grain boundary phases. *J Mater Sci Mater Electron*. 1992;3(2):93–101.
2. Jackson TB, Virkar AV, More KL, Dinwiddie RB, Cutler RA. High-thermal-conductivity aluminum nitride ceramics: the effect of thermodynamic, kinetic, and microstructural factors. *J Am Ceram Soc*. 1997;80(6):1421–35.
3. de Baranda PS, Knudsen AK, Ruh E. Effect of yttria on the thermal conductivity of aluminum nitride. *J Am Ceram Soc*. 1994;77(7):1846–50.
4. Prashant Reddy G, Gupta N. Material selection for microelectronic heat sinks: An application of the Ashby approach. *Mater Des*. 2010;31(1):113–7.
5. Yin L, Yang L, Yang W, Guo Y, Ma K, Li S, et al. Thermal design and analysis of multi-chip LED module with ceramic substrate. *Solid State Electron*. 2010;54(12):1520–4.
6. Jeong MW, Jeon SW, Lee SH, Kim Y. Effective heat dissipation and geometric optimization in an LED module with aluminum nitride (AlN) insulation plate. *Appl Therm Eng*. 2015;76:212–9.
7. Krnel K, Kosmač T. Reactivity of aluminum nitride powder in dilute inorganic acids. *J Am Ceram Soc*. 2000;83(6):1375–8.
8. Bowen P, Highfield JG, Mocellin A, Ring TA. Degradation of aluminum nitride powder in an aqueous environment. *J Am Ceram Soc*. 1990;73(3):724–8.
9. Fukumoto S, Hookabe T, Tsubakino H. Hydrolysis behavior of aluminum nitride in various solutions. *J Mater Sci*. 2000;35(11):2743–8.
10. Bartel CJ, Muhich CL, Weimer AW, Musgrave CB. Aluminum nitride hydrolysis enabled by hydroxyl-mediated surface proton hopping. *ACS Appl Mater Interfaces*. 2016;8(28):18550–9.

11. Slack GA. Nonmetallic crystals with high thermal conductivity. *J Phys Chem Solids*. 1973;34(2):321–35.
12. Slack GA, Tanzilli RA, Pohl RO, Vandersande JW. The intrinsic thermal conductivity of AlN. *J Phys Chem Solids*. 1987;48(7):641–7.
13. Troczynski TB, Nicholson PS. Effect of additives on the pressureless sintering of aluminum nitride between 1500° and 1800 °C. *J Am Ceram Soc*. 1989;72(8):1488–91.
14. Molisani AL, Yoshimura HN, Goldenstein H. Sintering mechanisms in aluminum nitride with Y or Ca-containing additive. *J Mater Sci Mater Electron*. 2009;20(1):1-8.
15. Molisani AL, Yoshimura HN, Goldenstein H, Watari K. Effects of CaCO<sub>3</sub> content on the densification of aluminum nitride. *J Eur Ceram Soc*. 2006;26(15):3431–40.
16. Streicher E, Chartier T, Boch P, Denanot M-F, Rabier J. Densification and thermal conductivity of low-sintering-temperature AlN materials. *J Eur Ceram Soc*. 1990;6(1):23–9.
17. Olhero SM, Miranzo P, Ferreira JMF. AlN ceramics processed by aqueous slip casting. *J Mater Res*. 2011;21(10):2460–9.
18. Liu Y, Zhou H, Wu Y, Qiao L. Improving thermal conductivity of aluminum nitride ceramics by refining microstructure. *Mater Lett*. 2000;43(3):114–7.
19. Molisani AL, Goldenstein H, Yoshimura HN. The role of CaO additive on sintering of aluminum nitride ceramics. *Ceram Int*. 2017;43(18):16972–9.
20. Watari K, Valecillos MC, Brito ME, Toriyama M, Kanzaki S. Densification and thermal conductivity of AlN doped with Y<sub>2</sub>O<sub>3</sub>, CaO, and Li<sub>2</sub>O. *J Am Ceram Soc*. 1996;79(12):3103-8.
21. Weimer AW. Particle atomic layer deposition. *J Nanopart Res*. 2019;21(1):9.
22. Hoskins AL, Coffey AH, Musgrave CB., Weimer AW. Nanostructured mullite steam oxidation resistant coatings for silicon carbide deposited via atomic layer deposition. *J Am Ceram Soc*. 2018;101(6):2493-505.
23. Bull SK, McNeary WW, Adkins CA, Champ TA, Hill CA, O'Brien RC, et al. Atomic layer deposition of tungsten nitride films as protective barriers to hydrogen. *Appl Surf Sci*. 2020;507:145019.
24. King DM, Spencer JA, Liang X, Hakim LF, Weimer AW. Atomic layer deposition on particles using a fluidized bed reactor with in situ mass spectrometry. *Surf Coat Technol*. 2007;201(22):9163-71.
25. Dokmai V, Methaapanon R, Pavarajarn V. Corrosion of amorphous alumina in deionized water under mild condition. *Appl Surf Sci*. 2020;499:143906.
26. Alexander GB, Heston WM, Iler RK. The solubility of amorphous silica in water. *J Phys Chem*. 1954;58(6):453-5.

**How to cite this article:** O'Toole RJ, Hill C, Buur PJ, Bartel CJ, Gump CJ, Musgrave CB, et al. Hydrolysis protection and sintering of aluminum nitride powders with yttria nanofilms. *J Am Ceram Soc*. 2022;1-5. <https://doi.org/10.1111/jace.18310>